

# Enhancement of photoelectrical properties in polymer nanocomposites containing modified single-walled carbon nanotubes by conducting dendrimer

L. Valentini,<sup>a)</sup> F. Mengoni, I. Armentano, and J. M. Kenny

*Department of Civil and Environmental Engineering, Perugia University and INSTM NIPLAB Centre, Loc. Pentima Bassa, 05100 Terni, Italy*

L. Ricco, J. Alongi, M. Trentini, and S. Russo

*Department of Chemistry and Industrial Chemistry, University of Genova and INSTM NIPLAB Centre, Via Dodecaneso 31, 16146 Genova, Italy*

A. Mariani

*Department of Chemistry, University of Sassari and INSTM Local Unit, Via Vienna 2, 07100 Sassari, Italy*

(Received 19 October 2005; accepted 16 March 2006; published online 2 June 2006)

We report the photoinduced conductivity changes measured on a system composed of single-wall carbon nanotubes (SWNTs) modified by a semiconducting poly(amidoamine) dendrimer (PAMAMC) characterized by highly aromatic end groups. Under illumination hole injection into SWNTs prevails over the photoinjection of electrons from PAMAMC to SWNT holes, and film photoconductivity is observed. This system was incorporated as an electroactive component within a conducting polymer [poly(3-octylthiophene)], providing improvements in the photoelectrical properties of the composite. Such supramolecular structures consisting of dendrimer-functionalized carbon nanotubes provide the means for an approach toward the preparation of photoactive materials of high current interest. © 2006 American Institute of Physics. [DOI: 10.1063/1.2196147]

## I. INTRODUCTION

Following the determination of the unique physical properties of single-walled carbon nanotubes (SWNTs),<sup>1–4</sup> it is important to mention that, in general, it is still very difficult to obtain SWNTs with a satisfying structure allowing for possible technological applications. Indeed, SWNTs grow mainly in the form of ropes consisting of individual graphene cylinders that are held together by strong van der Waals forces. Their affinity to adhere to each other makes as-grown SWNTs insoluble in common solvents. Two of the key challenges that are in the way of realizing multifunctional nanostructures made out of carbon nanotubes are a reliable control over their surface chemistry (i.e., through either covalent or noncovalent modification), and dispersion in terms of length and diameter.

Supramolecular assembly, which combines the outstanding photophysical properties of SWNTs with the unique structural features of dendrimers, would generate fascinating studies in supramolecular chemistry and materials sciences. On this regard, it was previously demonstrated<sup>5–8</sup> how dendrimers containing C<sub>60</sub> play two major roles depending upon their architecture and functionalities: they increase the solubility of C<sub>60</sub> in organic solvents, and they isolate C<sub>60</sub> from the external environment such as oxygen. At this stage several key challenges arise around the possibility to substitute C<sub>60</sub> with SWNTs with donor or acceptor functions in these nanohybrids.

As we previously reported,<sup>9</sup> supramolecular semicon-

ducting dendrimeric structures consisting of commercial poly(amidoamine) modified by adding substituted naphthalenediimides as end groups<sup>9</sup> [poly(amidoamine) (PAMAMC)] noncovalently interacting with single-walled carbon nanotubes have been synthesized.

Here we report the study of the photoelectrical properties of this system in thin film transistor geometry and the incorporation of PAMAMC-modified SWNTs as an electroactive component within an organic conducting polymer in order to enhance the photoconductivity.

## II. EXPERIMENTAL DETAILS

SWNTs were obtained from Carboxlex Inc. and consisted of ≈70–90 vol % carbon as SWNTs of 50 nm–1 μm in length and 0.8–2 nm in diameter. Noticable amount of SWNTs bundles was found.

PAMAMC was a laboratory preparation synthesized by reaction between the amino terminal groups of a generation three dendritic poly(amidoamine) and the hydrochloride salt of a monoimide monoanhydride: details for the synthesis and reaction with poly(amidoamine) end groups are reported in the aforementioned Ref. 9 and in the original work.<sup>10</sup>

Noncovalent interactions between PAMAMC and SWNTs have been achieved by sonication of the two elements of the couple in a solvent for PAMAMC: a mixture 1:1 (vol/vol) of CH<sub>3</sub>OH and CHCl<sub>3</sub>. The sample was analyzed and used after centrifugation in order to remove undissolved SWNTs.

For the preparation of the nanocomposite, poly(3-octylthiophene) (P3OT) was purchased from Sigma-Aldrich

<sup>a)</sup>Electronic mail: mic@unipg.it

Co. P3OT (60 mg), was dissolved in 25 ml of  $\text{CH}_3\text{OH}/\text{CHCl}_3$  (1:1 vol/vol). The PAMAMC-SWNTs was then added to P3OT solution (1:1 w/w). The PAMAMC-SWNTs/P3OT blend was then sonicated for 2 h.

Scanning electron microscopy (SEM) micrographs of the samples were obtained by a Leo Stereoscan 440 microscope, while a Jeol Jem 2010 microscope was used for TEM analysis.

Atomic force microscopy (AFM) was carried out in tapping mode at room temperature in ambient conditions. Samples for the AFM study were prepared by depositing a drop of the solution of PAMAMC-SWNT/P3OT blend onto a glass that was then allowed to dry in vacuum ( $10^{-1}$  Pa) for 12 h.

The transport properties were measured in a thin-film transistor geometry. Source-drain electrodes were fabricated using e-beam lithography technique on a 250-nm-thick thermal silicon oxide on a Si wafer. The electrodes consisted of a 40 nm bottom layer of Al coated with 40-nm-thick layer of Au. The device geometry was fixed with the source-drain channel length of 8  $\mu\text{m}$  and channel width of 100  $\mu\text{m}$ . Two types of devices were prepared. The first device was obtained depositing PAMAMC from a  $\text{CH}_3\text{OH}/\text{CHCl}_3$  solution (4  $\mu\text{l}$ ) onto  $\text{SiO}_2/\text{Si}$  wafer with previously patterned electrical contacts. The second device was obtained by positioning a solution of PAMAMC-SWNTs in  $\text{CH}_3\text{OH}/\text{CHCl}_3$  (4  $\mu\text{l}$ ). We measured the source-drain current ( $I_{SD}$ ) as a function of the gate voltage ( $V_G$ ) under gate voltage sweep for both types maintaining the drain voltage fixed at 0.5 V. The conductivity was monitored as a function of exposure time to ultraviolet-visible (UV-vis) radiation obtained with a xenon lamp ( $230 \text{ nm} < \lambda < 700 \text{ nm}$ , intensity of 85  $\text{mW}/\text{cm}^2$ ).

The photoelectrical properties of PAMAMC-SWNTs and PAMAMC-SWNT/P3OT blends was monitored for on/off light illumination cycles as a function of exposure to UV-vis radiation. The electrical measurements in this case were performed on thin film geometry obtained by drop casting of the  $\text{CH}_3\text{OH}/\text{CHCl}_3$  solutions onto patterned electrical contacts (electrode distance 3  $\mu\text{m}$ ) at room temperature.

### III. RESULTS AND DISCUSSION

The SEM study of pristine SWNT network reveals a large number of cross-linked nanotube bundles [Fig. 1(a)]. The SEM micrograph of SWNT-modified PAMAMC [Fig. 1(b)] puts in evidence that the addition of dendrimer to carbon nanotubes leads to partial unrouting of SWNTs trapped in the PAMAMC matrix.

The inset of Fig. 1(b) compares a solution of pristine PAMAMC (A) and a solution of PAMAMC-modified SWNTs in  $\text{CH}_3\text{OH}/\text{CHCl}_3$  after centrifugation (B). From this image it is evident that the nanotubes are well dispersed in the sample B; no sedimentation has been observed even after ten days.

Moreover, the TEM observation (Fig. 2) allowed direct imaging of SWNT sidewalls showing the intimate interaction between PAMAMC and carbon nanotubes. Figure 2(a) shows clean sidewalls of pristine nanotubes, while the den-

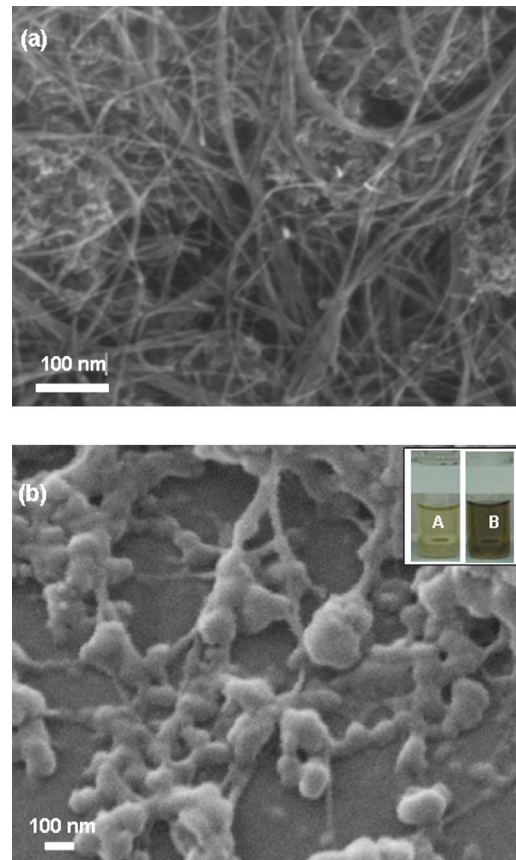


FIG. 1. (a) SEM image of a specimen of pristine SWNTs; (b) SEM micrograph of PAMAMC coating SWNTs. The inset shows the solubility in organic solvent: PAMAMC in  $\text{CH}_3\text{OH}/\text{CHCl}_3$  (A), PAMAMC-SWNTs in  $\text{CH}_3\text{OH}/\text{CHCl}_3$  (B).

dimer adsorption on SWNT sidewalls is responsible of the coating evidenced in Fig. 2(b) and of the solubilization phenomenon reported above.

Figure 3(a) shows the gate dependence of the conductance for the PAMAMC transistor light-on and light-off events. The time dependence (upper inset) reveals that, under illumination, the current at negative gate bias ( $p$  channel) remains unchanged while the current at positive gate bias ( $n$  channel) increases. The above results clearly show that the conducting dendrimer behaves like a  $n$ -type semiconductor.<sup>11</sup> The illumination results in the excitation of electrons to the conduction band, followed by a transfer of electrons from the conduction band to the defective, oxidized carbon sites.

Figure 3(b) plots the transistor characteristics for SWNT modified with PAMAMC. From  $I_{sd}$  vs  $V_g$  measurements, we found that the ensemble in the device appeared of  $p$  type, exhibiting an overall electrical conductance decrease when the gate voltage was swept from  $-10$  to  $10$  V. The nonelectrical depletion of FET device at positive gate voltage was due to the conduction of small percentages of metallic nanotubes in the ensemble. In this device, under UV-vis light, the increase of the current at negative biases is achieved at the expense of a slight current variation at positive bias current, which is due to  $p$ -type conduction (upper inset). It should be mentioned that (data not shown) a decrease of the  $p$  channel was observed for pristine SWNTs due to the oxygen photodesorption under illumination. The lower conductivity

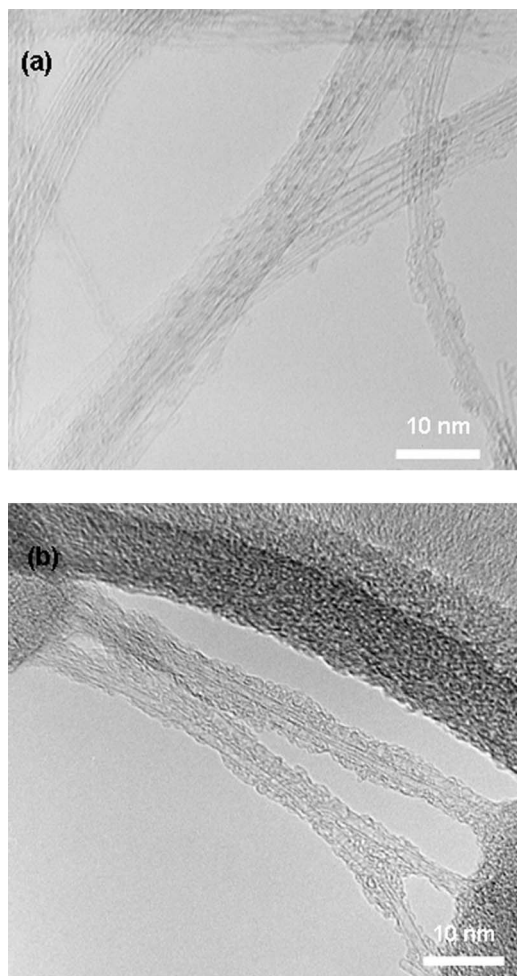


FIG. 2. (a) TEM micrograph of the specimen of pristine SWNTs and (b) TEM image of PAMAMC coating SWNTs.

of the PAMAMC-SWNT film with respect to neat PAMAMC, is due to the injection of electrons into the SWNT holes, which is a well-known phenomenon for bulk *p*-type semiconductors.<sup>12–15</sup> Visible illumination also generates holes in SWNT via a withdrawal of electrons from nanotubes by photoexcited PAMAMC. The increase of the *p*-type channel at negative gate biases observed in Fig. 3(b) is consistent with this mechanism. Thus, two processes occur under illumination of the hybrid system explaining why the photoconductivity of PAMAMC-modified SWNT film in Fig. 4 first increases and then, in darkness, decreases to values that are lower than they were before UV-vis exposure. In darkness, back-electron transfers from PAMAMC to SWNTs outnumber the photoinduced holes of the SWNTs.

With the view to construct supramolecular nanotube composite, whose properties could be of interest in nanotechnology (e.g., molecular switches and solar cells), we became interested in nanotube-containing conducting polymers.

Figure 5(a) shows an AFM phase image of a 70-nm-thick PAMAMC-SWNT/P3OT film. The phase image in tapping mode AFM gives information concerning the loss in energy of the tip upon contact with the surface. From the image in Fig. 5(a) it is apparent that there are two materials present, or at least two phases, evidenced by the darker and the lighter regions. We note that the length scale of phase

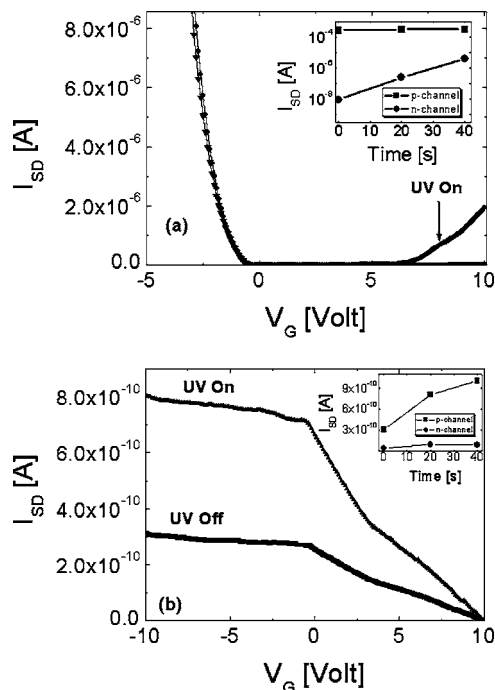


FIG. 3. (a) Gate dependence of the source-drain current ( $I_{SD}$ ) (drain voltage fixed at 0.5 V) under light-on and light-off steps for PAMAMC. Upper inset shows the time dependence of *p*-channel (averaged between  $-7$  and  $-10$  V gate voltage) and *n*-channel (averaged between  $+7$  and  $+10$  V gate voltage) current under illumination. (b) Gate dependence of the source-drain current ( $I_{SD}$ ) (drain voltage fixed at 0.5 V) under light-on and light-off steps for PAMAMC-modified SWNTs. Upper inset shows the time dependence of *p*-channel (averaged between  $-7$  and  $-10$  V gate voltage) and *n*-channel (averaged between  $+7$  and  $+10$  V gate voltage) current under illumination.

separation is of the order of 10 nm, matching the short exciton diffusion length in polymeric semiconductors. Contrary to what reported on Fig. 1(b), SEM analysis [Fig. 5(b)] performed on PAMAMC-SWNT/P3OT film demonstrates that the surface becomes almost uniform. Moreover, as reported in Fig. 5(c), the nanotubes onto PAMAMC-SWNTs/P3OT system show a “bumpy and spiky” material appearing on their sidewalls, underlining the good affinity between PAMAMC-SWNTs electroactive component and the conducting polymer.

A critical factor for improving the efficiency of solar cells is to match the photon flux spectrum from the sun with the absorption of the donor/acceptor blend.<sup>16–18</sup>

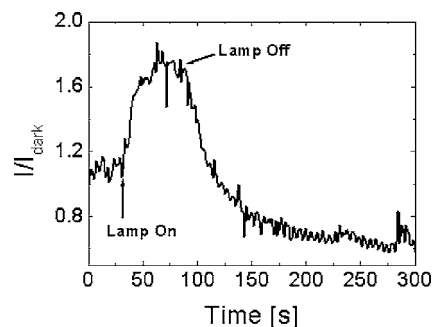


FIG. 4. Evolution of the PAMAMC-SWNT film normalized current ( $I_{\text{dark}}$  is the initial resistance of the sample in darkness) under light-on and light-off steps.

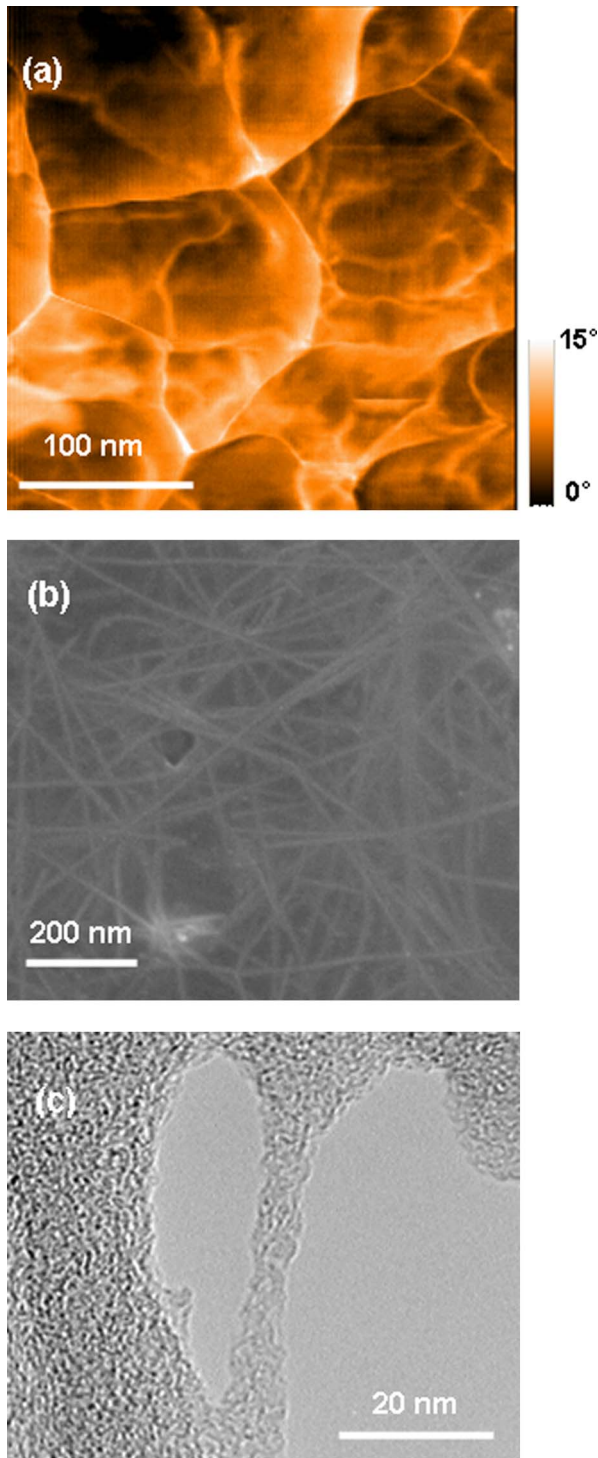


FIG. 5. (Color online) (a) AFM phase image of a 70 nm PAMAMC-SWNT/P3OT film deposited onto a glass substrate. (b) SEM image of a PAMAMC-SWNT/P3OT film deposited onto a glass substrate. (c) TEM image of a PAMAMC-SWNT/P3OT blend.

The UV-vis spectrum of the pristine PAMAMC, the P3OT polymer and the PAMAMC-SWNT/P3OT (1:1, w/w) blend in thin films is shown in Fig. 6. The PAMAMC and P3OT alone exhibit significant absorptions into the UV and visible region, respectively. PAMAMC-SWNT/P3OT blend exhibits a very wide absorption range, with the absorption peaks of the blend at about 365–382 nm, which corresponds to the PAMAMC. Going from pristine PAMAMC and P3OT

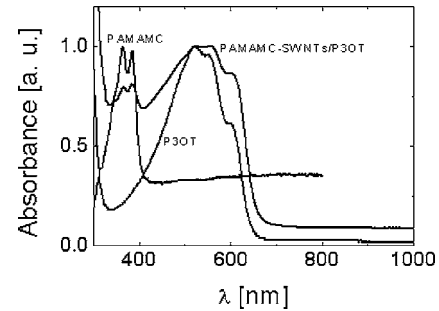


FIG. 6. Normalized UV-vis absorption of the pristine PAMAMC, P3OT polymers and the blend of PAMAMC-SWNT/P3OT (1:1, w/w), in thin films drop-cast from  $\text{CH}_3\text{OH}/\text{CHCl}_3$  onto glass.

to composite sample, no signal appears and the typical peaks do not undergo any shift, although a difference in their intensity is evident. This change together with the AFM image [Fig. 5(a)] suggests modifications in the electronic structure of P3OT as a consequence of PAMAMC-SWNT introduction.

The typical photoelectrical response of PAMAMC-SWNTs and PAMAMC-SWNT/P3OT blend in thin films for the on/off light illumination cycles in air is shown in Fig. 7. The main feature in the photoelectrical temporal behavior of interest is a fast rise/decay of the photocurrent in response to the on/off illumination step together with an enhanced decrease of resistance for the PAMAMC-SWNT/P3OT blend under illumination. Notably, the stability of the photocurrents to on/off cycling shows a moderate change both for the PAMAMC-SWNT/P3OT blend and for the PAMAMC-SWNT sample. These observations are presumably consistent with an  $\text{O}_2$  photodesorption as the main cause of the photocurrent changes. We cannot rule this effect out, and it is currently under investigation. In the inset of Fig. 7 the photoelectrical response for SWNTs modified by P3OT is also reported. Even if the conductivity is higher, it is evident how the “on” current variation is lower than that of the PAMAMC-SWNT/P3OT blend, with the photoelectrical response that shows a relaxation time.

#### IV. CONCLUSIONS

In conclusion, SWNTs with noncovalently linked conducting dendrimer have been prepared and characterized as

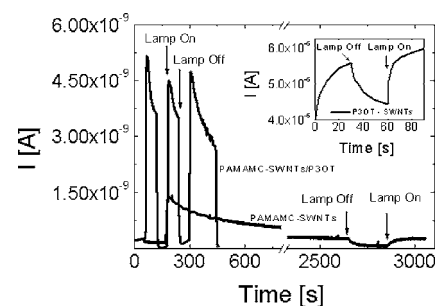


FIG. 7. Temporal photoelectrical current response of PAMAMC-SWNTs and PAMAMC-SWNT/P3OT blends in thin films with on/off step illumination in air. For the PAMAMC-SWNT hybrid system the lamp was switched on at about 150 s and switched off at about 2600 s. The inset shows the temporal photoelectrical current response of P3OT-SWNT blend in thin films with on/off step illumination in air.

potential supramolecular donor-acceptor complexes. We have achieved the control over the active components of organic optoelectronic devices using conducting polymer and self-organization of hybrid materials. We consider this to be a general and widely applicable strategy for controlled assembly of photoactive structures.

## ACKNOWLEDGMENTS

The authors gratefully acknowledge the financial support from the National Consortium of Materials Science and Technology (INSTM) through the NANOFUN-POLY Network of Excellence. This work was carried out also with the financial support from the MIUR (PRIN 2003, prot. 2003093440).

<sup>1</sup>S. Iijima, *Nature (London)* **56**, 354 (1991).

<sup>2</sup>C. N. R. Rao, B. C. Satishkumar, A. Govindaraj, and M. Nath, *ChemPhysChem* **2**, 78 (2001).

<sup>3</sup>S. S. Xie, B. H. Chang, W. Z. Li, Z. W. Pan, L. F. Sun, J. M. Mao, X. H.

Chen, L. X. Qian, and W. Y. Zhou, *Adv. Mater. (Weinheim, Ger.)* **11**, 1135 (1999).

<sup>4</sup>P. M. Ajayan, *Chem. Rev. (Washington, D.C.)* **99**, 1787 (1999).

<sup>5</sup>J.-F. Nierengarten, *Chem.-Eur. J.* **6**, 3667 (2000); J.-F. Nierengarten, N. Armaroli, G. Accorsi, Y. Rio, and J.-F. Eckert, *ibid.* **9**, 37 (2003).

<sup>6</sup>L. Echegoyen and L. E. Echegoyen, *Acc. Chem. Res.* **31**, 593 (1998).

<sup>7</sup>D. M. Guldi, *Chem. Commun. (Cambridge)* **5** 321 (2000).

<sup>8</sup>K. L. Wooley, C. J. Hawker, J. M. J. Fréchet, F. Wudl, G. Srdanov, S. Shi, C. Li, and M. Kao, *J. Am. Chem. Soc.* **115**, 9836 (1993).

<sup>9</sup>L. Valentini, I. Armentano, L. Ricco, J. Alongi, G. Pennelli, A. Mariani, S. Russo, and J. M. Kenny, *Diamond Relat. Mater.* **15**, 95 (2006).

<sup>10</sup>I. Tabakovic, L. L. Miller, R. G. Duan, D. Tully, and D. A. Tomalia, *Chem. Mater.* **9**, 736 (1997).

<sup>11</sup>M. E. Itkis, D. E. Perea, S. Niyogi, S. M. Hamon, M. A. Hu, H. Zhao, and B. Haddon, *Nano Lett.* **3**, 309 (2003).

<sup>12</sup>S. Kazaoui, N. Minami, H. Kataura, and Y. Achiba, *Synth. Met.* **121**, 1201 (2001).

<sup>13</sup>F. Hennrich, R. Wellmann, S. Malik, S. Lebedkin, and M. M. Kappes, *Phys. Chem. Chem. Phys.* **5**, 178 (2003).

<sup>14</sup>L. S. Darken and S. A. Hyder, *Appl. Phys. Lett.* **42**, 731 (1983).

<sup>15</sup>C. Winder and N. S. Sariciftci, *J. Mater. Chem.* **14**, 1077 (2004).

<sup>16</sup>C. J. Brabec, *Sol. Energy Mater. Sol. Cells* **83**, 273 (2004).

<sup>17</sup>R. J. Chen, N. R. Franklin, J. Kong, J. Cao, T. W. Tomblor, Y. Zhang, and H. Dai, *Appl. Phys. Lett.* **79**, 2258 (2001).

<sup>18</sup>M. Shim and G. P. Siddons, *Appl. Phys. Lett.* **83**, 3564 (2003).